

# REPORT DOCUMENTATION PAGE

Form Approved  
OMB No. 0704-0188

Public reporting burden for this collection of information is estimated to average 1 hour per response, including the time for reviewing instructions, searching existing data sources, gathering and maintaining the data needed, and completing and reviewing this collection of information. Send comments regarding this burden estimate or any other aspect of this collection of information, including suggestions for reducing this burden to Department of Defense, Washington Headquarters Services, Directorate for Information Operations and Reports (0704-0188), 1215 Jefferson Davis Highway, Suite 1204, Arlington, VA 22202-4302. Respondents should be aware that notwithstanding any other provision of law, no person shall be subject to any penalty for failing to comply with a collection of information if it does not display a currently valid OMB control number. **PLEASE DO NOT RETURN YOUR FORM TO THE ABOVE ADDRESS.**

<b>1. REPORT DATE (DD-MM-YYYY)</b> 15-08-2017		<b>2. REPORT TYPE</b> Technical Paper		<b>3. DATES COVERED (From - To)</b> 15-08-2016 – 15-08-2017	
<b>4. TITLE AND SUBTITLE</b>  Using a Double-Well Oscillator to Train Binary Neural Networks				<b>5a. CONTRACT NUMBER</b> N/A	
				<b>5b. GRANT NUMBER</b> N/A	
				<b>5c. PROGRAM ELEMENT NUMBER</b> N/A	
<b>6. AUTHOR(S)</b>  1st Lt Aron Wing, USAF; Rose Rustowicz				<b>5d. PROJECT NUMBER</b> N/A	
				<b>5e. TASK NUMBER</b> N/A	
				<b>5f. WORK UNIT NUMBER</b> N/A	
<b>7. PERFORMING ORGANIZATION NAME(S) AND ADDRESS(ES)</b> Air Force Research Laboratory Information Directorate 525 Brooks Road, Rome, NY 13441				<b>8. PERFORMING ORGANIZATION REPORT NUMBER</b>	
<b>9. SPONSORING / MONITORING AGENCY NAME(S) AND ADDRESS(ES)</b>  N/A				<b>10. SPONSOR/MONITOR'S ACRONYM(S)</b> N/A	
				<b>11. SPONSOR/MONITOR'S REPORT NUMBER(S)</b> N/A	
<b>12. DISTRIBUTION / AVAILABILITY STATEMENT</b>  DISTRIBUTION A; Distribution is unlimited					
<b>13. SUPPLEMENTARY NOTES</b> N/A					
<b>14. ABSTRACT</b>  Certain processors specifically designed for neural networks are defined with low-precision weights and activations. Low-precision weights and activations can considerably reduce the power required for computing a neural network. Although the neural network is still capable of generalizing the data to determine relevant features, the loss of precision in the values sometimes results in considerable loss of test accuracy. In this paper, we explore using a dynamical system which introduces transient chaos to the loss function that helps train binary network layers. Implementing theoretical stochastic rounding probabilities on the MNIST data set we improved the test error to state of the art for a binary network. We also show that adding a dynamical equation to the loss function of a network can effectively binarize a network.					
<b>15. SUBJECT TERMS</b>					
<b>16. SECURITY CLASSIFICATION OF:</b> UNCLASSIFIED			<b>17. LIMITATION OF ABSTRACT</b> Distribution A	<b>18. NUMBER OF PAGES</b> 19	<b>19a. NAME OF RESPONSIBLE PERSON</b> Aron Wing
<b>a. REPORT</b> UNCLASSIFIED	<b>b. ABSTRACT</b> UNCLASSIFIED	<b>c. THIS PAGE</b> UNCLASSIFIED			<b>19b. TELEPHONE NUMBER (include area code)</b> (315) 330-4424

Standard Form 298 (Rev. 8-98)  
Prescribed by ANSI Std. Z39.18

# Using a Double-Well Oscillator to Train Binary Neural Network Layers

2d Lt Aron Wing

Miss Rose Rustowicz

Air Force Research Laboratory- Information Directorate

15 August 2017

## Abstract

Certain processors specifically designed for neural networks are defined with low-precision weights and activations. Low-precision weights and activations can considerably reduce the power required for computing a neural network. Although the neural network is still capable of generalizing the data to determine relevant features, the loss of precision in the values sometimes results in considerable loss of test accuracy. In this paper, we explore using a dynamical system which introduces transient chaos to the loss function that helps train binary network layers. Implementing theoretical stochastic rounding probabilities on the MNIST data set we improved the test error to state of the art for a binary network. We also show that adding a dynamical equation to the loss function of a network can effectively binarize a network.

## 1 Introduction

### 1.1 Motivation

The equation for this paper was developed in order to provide a means with which one could entice activations of neurons in a neuromorphic machine learning algorithm to have binary representations. Neuromorphic processors do not have the floating point precision of GPUs and instead rely on generalizing feature spaces to predict classifications. These feature spaces are transduced from the original format to a processor specific readable format. In this paper the desired format is binary. Because of this motivation we assume the initial conditions of the system have been normalized between 0 and 1 and we will analyze the system using a dense uniform distribution of initial conditions to provide global dynamics without loss of generality.

### 1.2 Initial System Set-Up

The idea is that if we add error to the system for not having a binary representation, then we may be able to entice it to the desired representation. We began by finding an equation for which one could define the y-axis as the error we will add to the system and the x-axis as the value of an activation or weight in the system. Since we want to entice the activations to train toward binary, we want the error introduced by the equation to be minimum at 0 and 1. We hope that by doing this, the machine learning algorithms will train the values to the lowest error and therefore near 0

or 1. We also wanted to ensure that the system is defined for all values and that the system is smooth and continuous. There are many possibilities, but we started with the simplest one that came to mind:

$$f(x) = (x)(x - 1)(2x - 1) \quad \text{Equation 1.1}$$

However, it is clear from figure 1.1 that for every x this system does nothing but round to either 0 or 1. Taking the integral:

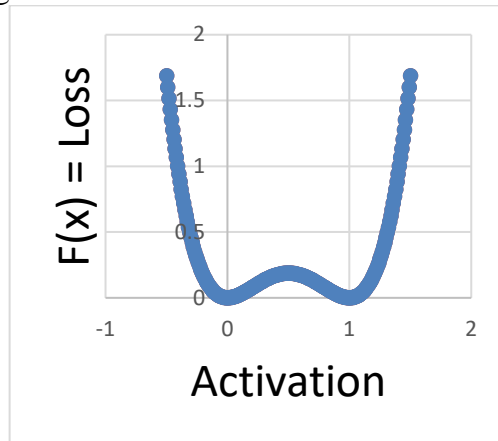


Fig. 1.1

Note: One can naively determine the end-state dynamics of this system by imagining rain drops falling on the figure and rolling down-hill to the bottom of the wells

In order to develop more complicated system behavior, we introduced two new states to the system, namely:

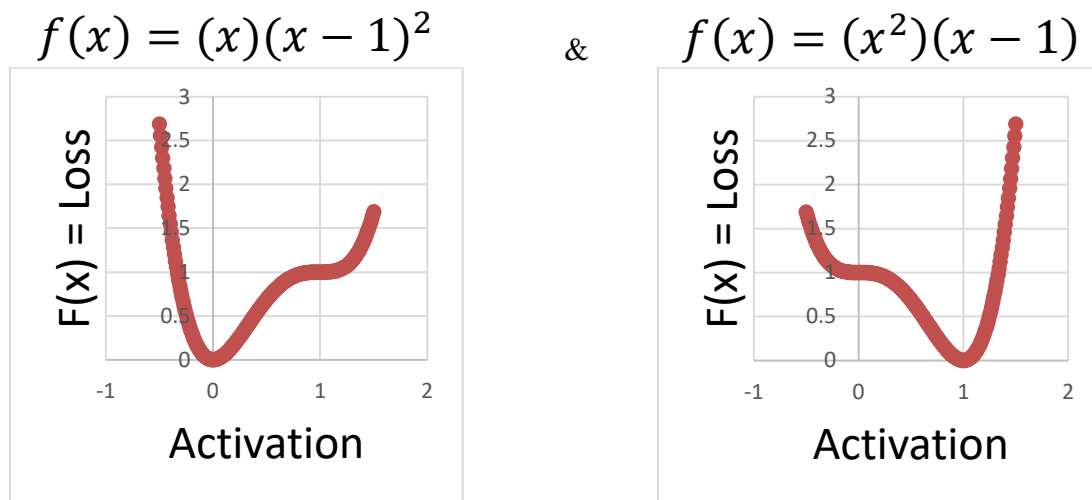


Fig. 1.2

Figure 1.2: These states allow for the system to reach 0 or 1, respectively, for any initial condition. These three states were combined to provide the following two variable dynamical equation:

$$f(x, t) = h((x)(x - 1)(2x + \sin(t) - 1))$$

Integrating represents the error introduced by our system. We have obtained our desired system where  $H = \frac{h}{6}$  controls the “peakiness” of the system and  $t$  is a free time-parameter that oscillates the “hill” across the system. We will progress  $t$  as a function of the step during training of a machine learning algorithm.  $C$  is a control parameter used to maintain the structure of the system. That is,  $C = \frac{h}{6} * \sin(t)$  if  $\sin(t) > 0$  else  $C = 0$ . The amount defined by equation 1.3 will be the amount of error we introduce.

$$F(x, t) = H(x)^2 [(2x - 3) \sin(t) + 3((x - 1)^2)] + C \quad \text{Equation 1.3}$$

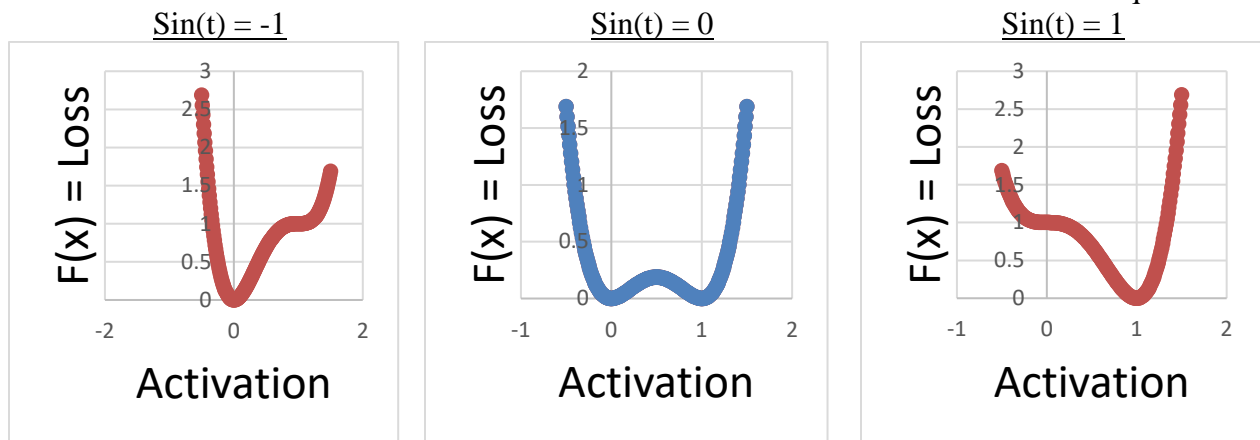


Fig. 1.3

### 1.3 Initial Observations

We have constructed a system defined by equation 1.3 which we call a modified double-well oscillator.

- (1) It is obvious from this construction that 0 and 1 are, generally, stable orbits of the system. If the free parameter  $t$  is slow the system will predictably approach the stable orbits of 0 or 1 as the system “sloshes” back-and-forth.
- (2) If the parameter  $H$  is too large, the “sloshing” will be extreme and the system will become unstable.

### 1.4 Initial Questions

- (1) Is this system always predictable, that is does there exist sensitive dependence on the initial conditions (SDIC)?
- (2) How large is “too” large for parameter  $h$ ?
- (3) Are there parameters for which there exists chaos?
- (4) Can this function be added to the loss function, or error, of a neural network to train binary layers?

## 2 Modeling and Simulation

All following simulations in this paper were conducted using a first order Euler approximation map to the system. That is

$$x_{n+1} = x_n - \varepsilon f(x_n, t_n) \quad \text{Equation 2.1}$$

Where  $f$  is equation 1.2,  $\varepsilon = .01$  and  $tStep = t_{n+1} - t_n$ , so that

$$x_{n+1} = x_n - \varepsilon h((x_n)(x_n - 1)(2x_n + \sin(t_n) - 1)) \quad \text{Equation 2.2}$$

Note that, the selection of different epsilon is not necessary as it is  $h$  and  $tStep$  that dominate the dynamical behavior of this system; that is, we could always set a constant  $\alpha$  and let  $\varepsilon = E\alpha$  then setting  $h := \frac{h}{E}$  returns equation 2.1 with epsilon fixed at  $\alpha$ . The overall dynamics will be conserved, just the values of  $h$  for which they occur will change. Whenever we refer to  $F$ , or Equation 1.3 from this point on in this paper, we mean the approximation based on Equation 2.2.

Notation presented in this paper:  $x^i_j$  refers to the  $i^{\text{th}}$  activation or weight at the  $j^{\text{th}}$  step.

## 2.1 Initial Observation Simulations

First we let the initial value of  $t$ ,  $t(0)$ , and  $tStep$  be constants and raised the “peakiness” parameter,  $h$ , slowly until the dynamics of the system change.

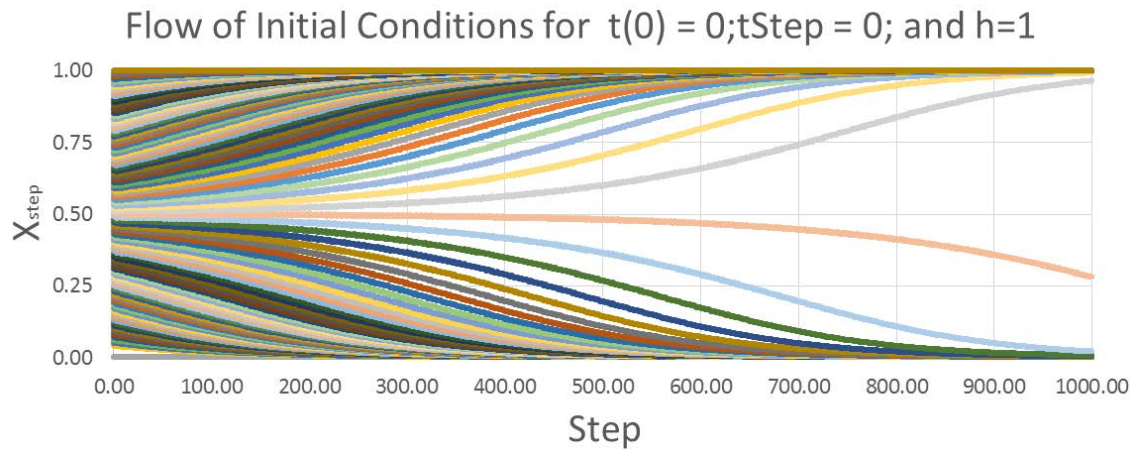


Fig. 2.1

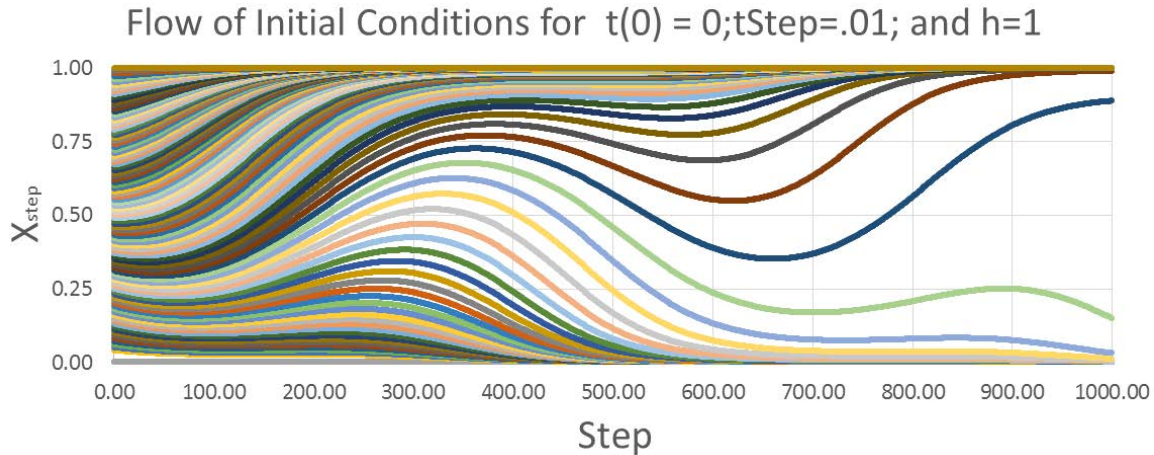


Fig. 2.2

Figures 2.1 and 2.2 show that for small  $t$  and  $h$ , all initial conditions approach the stable orbits 0 or 1 predictably based on how  $t$  is initialized. However, if we continue to increase  $h$  the behavior of the system will become unstable. We did not prove, but feel it is safe to assume based on simulation, that there exists some  $t(0)$  and  $tStep$  values for which  $x^i_\infty$  approaches  $\pm\infty$ . Section 3 explores the stable regions of  $F$  in more detail.

## 2.2 Initial Questions Simulations

This section will begin to explore system stability which will lead into system states for which there exists SDIC, chaos and transient chaos. We slowly let  $h$  grow we noticed that the system dynamics did not differ from figures 2.1 and 2.2 until around  $h = 75$  where the trajectories begin to peak over the stable orbits at 0 and 1. However, at  $h = 75$  the end state is still predictable and there are no periodic orbits (see figure 2.3). The system maintains this structure until about  $h = 160$  where the trajectories peak over the stable orbits, then oscillate back across to the opposite attractor (see figure 2.4). It is at about  $h = 160$  that the system begins to exhibit SDIC (see figure 2.5). Through simulation we determine that the maximum  $h$  for any random  $t(0)$  and  $tStep$  is approximately 190.5

Although the dynamics have changed considerably and have shown signs of transient chaos (fig. 2.5), the stable orbits at 0 and 1 still dominate in the system and attract all trajectories as stable points. This behavior goes away around  $h=170$  when the system begins to generate period 8 stable orbits around 0 and 1 for  $tStep = \pi/2$  (see figure 2.6). 53 of 100 trajectories from randomly initialized conditions are shown in figure 2.6; the other 47 trajectories have period 8 orbits around the stable orbit at 1.

Flow of Initial Conditions for  
 $t(0)=4.47314161082;tStep=5.68662579515;h=75$

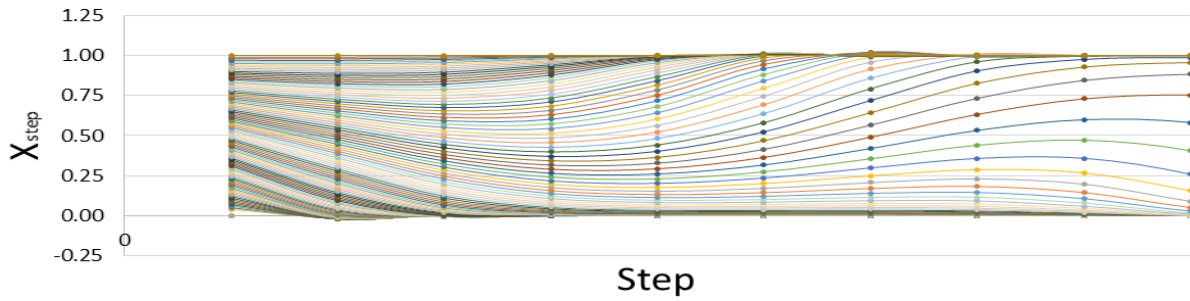


Fig. 2.3 Stable predictable flow

Flow of Initial Conditions for  
 $t(0)=3.681338382771;tStep=1.09013595992;h=160$

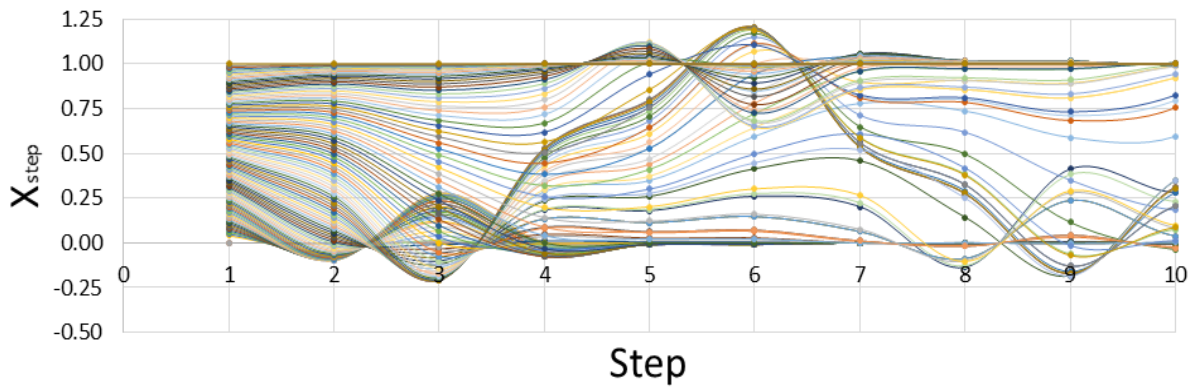


Fig. 2.4 Oscillating Dynamic Flow

Flow of Initial Conditions for  
 $t(0)=5.92641363356;tStep=1.6786358618;h=160$

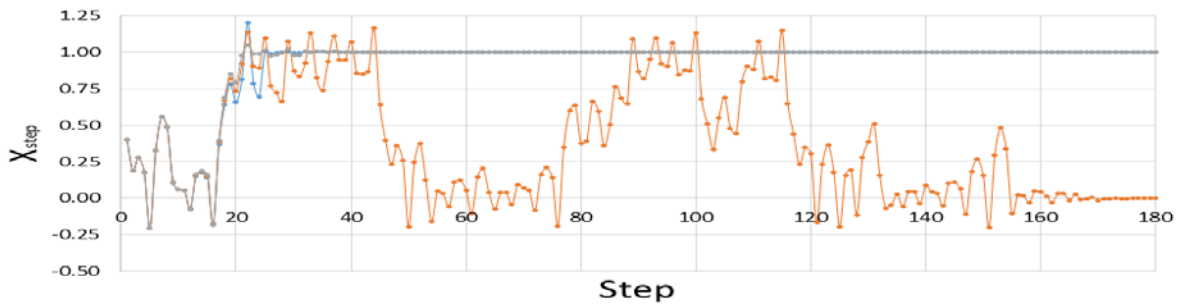


Fig. 2.5 SDIC  $x^1_0 = .4010$   $x^2_0 = .4011$  and  $x^3_0 = .4012$

	$x^1_0 = .42$	$x^2_0 = .43$	$x^3_0 = .44$	$x^4_0 = .45$
Step	$x_{step}$	$x_{step}$	$x_{step}$	$x_{step}$
<b>984</b>	<b>-0.0078819528</b>	<b>0.0095668443</b>	<b>0.9927510065</b>	<b>0.9927510065</b>
985	-0.0075566346	0.0097409521	1.0169397068	1.0169397068
986	0.0072489935	-0.0084494277	0.9904331557	0.9904331557
987	-0.0169397068	0.0206455587	0.9902590479	0.9902590479
988	0.0095668443	-0.0078819528	1.0084494277	1.0084494277
989	0.0097409521	-0.0075566346	0.9793544413	0.9793544413
990	-0.0084494277	0.0072489935	1.0078819528	1.0078819528
991	0.0206455587	-0.0169397068	1.0075566346	1.0075566346
<b>992</b>	<b>-0.0078819528</b>	<b>0.0095668443</b>	<b>0.9927510065</b>	<b>0.9927510065</b>
993	-0.0075566346	0.0097409521	1.0169397068	1.0169397068
994	0.0072489935	-0.0084494277	0.9904331557	0.9904331557
995	-0.0169397068	0.0206455587	0.9902590479	0.9902590479
996	0.0095668443	-0.0078819528	1.0084494277	1.0084494277
997	0.0097409521	-0.0075566346	0.9793544413	0.9793544413
998	-0.0084494277	0.0072489935	1.0078819528	1.0078819528
999	0.0206455587	-0.0169397068	1.0075566346	1.0075566346
<b>1000</b>	<b>-0.0078819528</b>	<b>0.0095668443</b>	<b>0.9927510065</b>	<b>0.9927510065</b>

Table2.1

Flow of Initial Conditions for  
 $t(0)=3.27071673804;tStep=\pi/2;h=170$

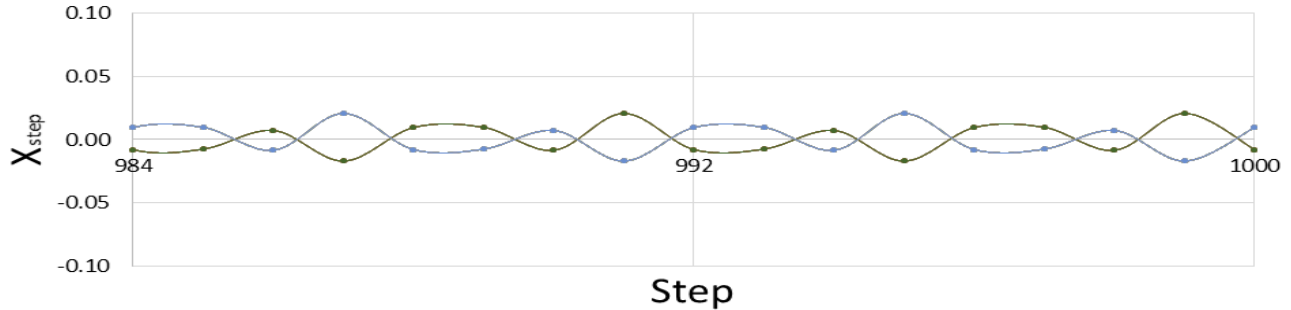


Fig. 2.6 Pictured are 53 unique initial condition trajectories period-8 oscillating around 0 (see table 2.1).

Flow of Initial Conditions for  $t(0)=0;tStep=0;h=250$

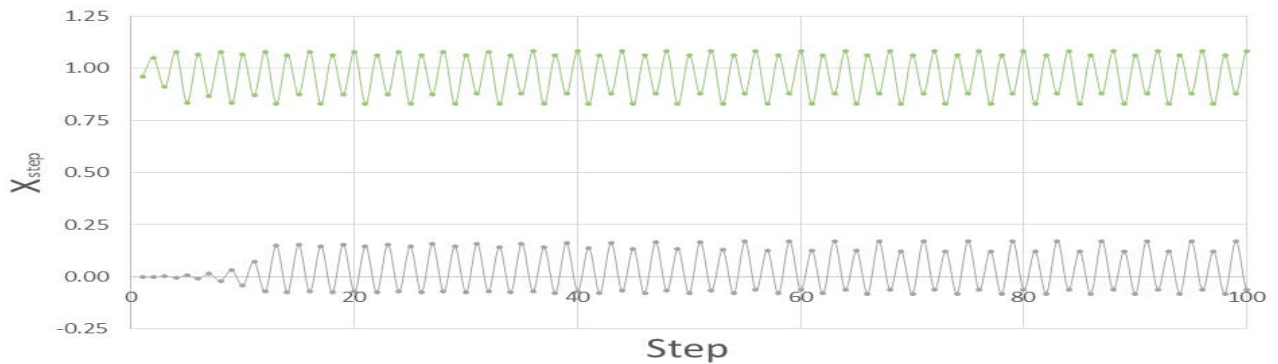


Fig. 2.7 with initial conditions  $x^1_0 = .0012$  and  $x^2_0 = .97$

Figure 2.7 and table 2.2 shows the rise of period-4 oscillations in the for  $h = 250$ . Note that, as shown in table 2.2, every initial condition will reach a steady state of period 4 oscillations  $\{-.08, .17, -.06, .12\}$  if  $x_0 < .5$  or  $\{1+.08, 1-.17, 1+.06, 1-.12\} = \{1.08, .83, 1.06, .88\}$  if  $x_0 > .5$ .

Step	$x_{step}^{1_0 = .61}$	$x_{step}^{2_0 = .72}$
<b>991</b>	<b>0.877572856879239</b>	<b>1.061760827832230</b>
992	1.080402612634390	0.877572856879239
993	0.828312884504610	1.080402612634390
994	1.061760827832230	0.828312884504610
<b>995</b>	<b>0.877572856879239</b>	<b>1.061760827832230</b>
996	1.080402612634390	0.877572856879239
997	0.828312884504610	1.080402612634390
998	1.061760827832230	0.828312884504610
<b>999</b>	<b>0.877572856879239</b>	<b>1.061760827832230</b>
1000	1.080402612634390	0.877572856879239

Table 2.2

Flow of Initial Conditions for  $t(0)=0;tStep=0;h=250$

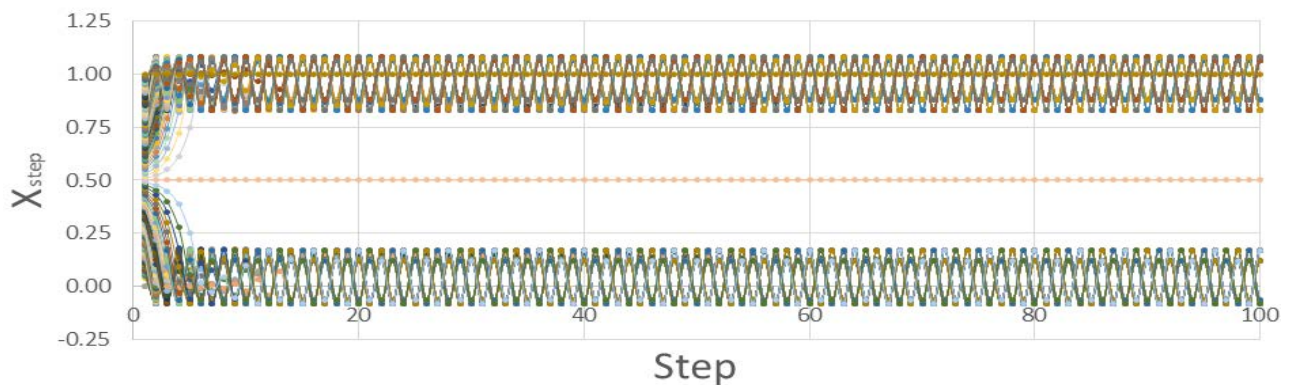


Fig. 2.8

Flow of Initial Conditions for  $t(0)=0;tStep=0;h=250$

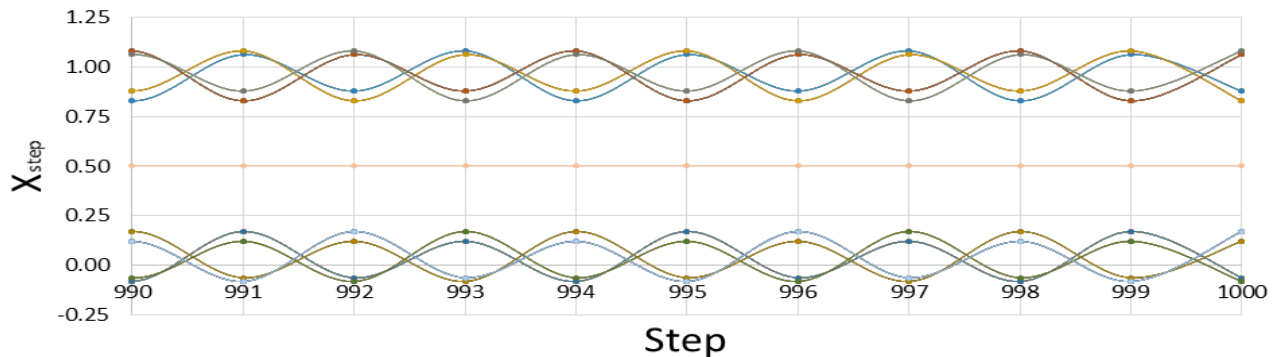


Fig. 2.9

Figures 2.8 and 2.9 show the propagation of 100 unique conditions stabilizing to harmonious period 4 orbits. However, adding a small change to tStep the system in this intermediate range of h brings rise to the question of sensitive dependence on initial conditions. Figures 2.10 and 2.11 show the system beginning to destabilize and exhibit some aperiodic behavior. Although both figures eventually settle to a stable orbit we question the conditions under which the 0 and 1 attractors will dominate the system. If tStep is increased further the system will destabilize completely and initial conditions will escape to infinity.

Flow of Initial Conditions for  $t(0)=0;tStep=.001;h=250$

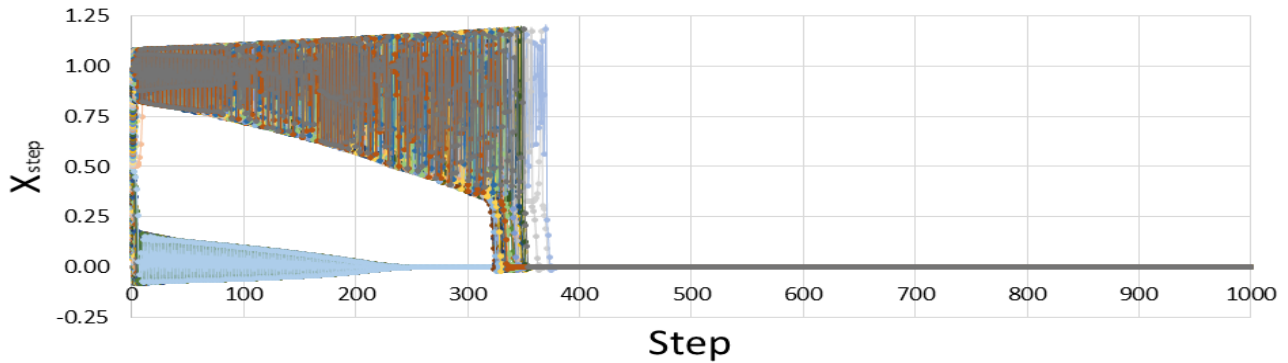


Fig. 2.10

Flow of Initial Conditions for  $t(0)=0;tStep=\pi-.001;h=250$

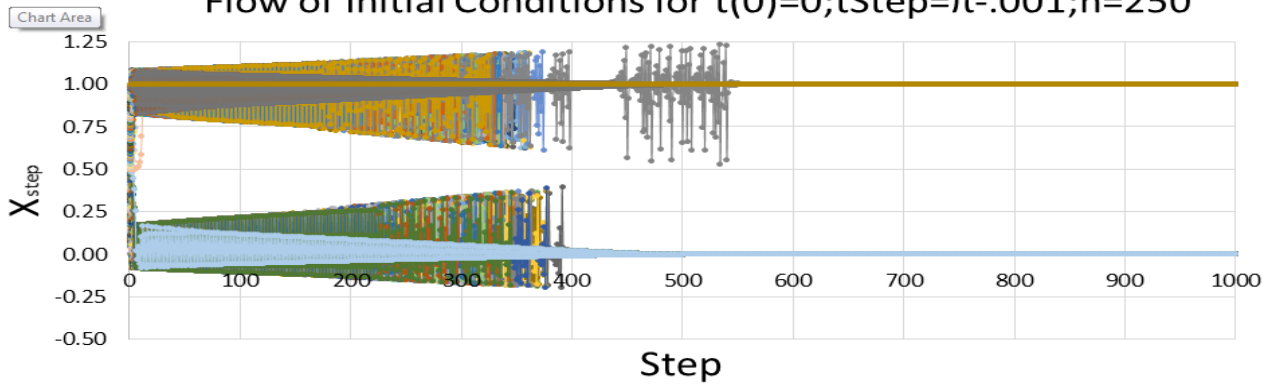


Fig. 2.11

Up to now we have seen that eventually all the trajectories will settle at or oscillate about the stable points or stable orbits at 0 or 1. However if we set h to the globally stable max around 190.5 and choose tStep as  $\pi/2$  we will see a new behavior emerge.

Flow of Initial Conditions for  $t(0)=0;tStep=\pi/2;h=190.5$

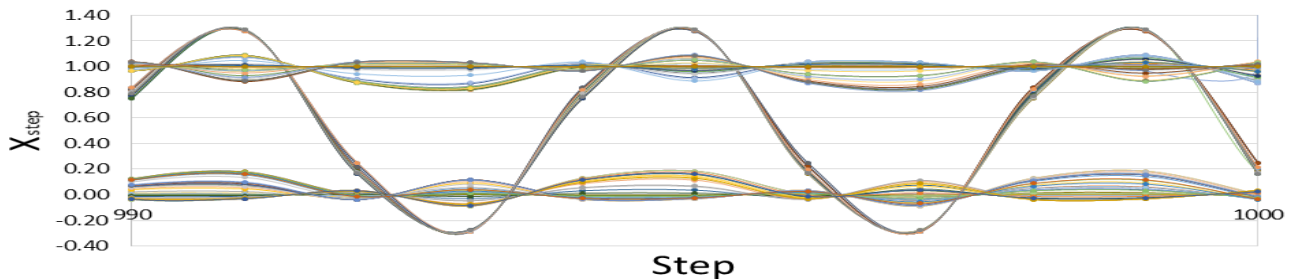


Fig. 2.12

The system is now overall still stable, but the 0 and 1 attractors no longer dominate the system, as shown in figure 2.12. The paper has concluded with simulating the initial observations and is now poised to begin answering the initial questions. Of primary concern is determining the valid ranges of  $tStep$  and  $h$  for which the system is always stable. This will naturally lead us down a road to discovery answering the remaining questions.

### 3 Chaotic Behavior

Continuing on our path of discovery we set  $h$  to a locally stable max of 205. Here, we notice that the orbits 0 and 1 have completely destabilized, but the system overall remains stable with trajectories that fill the space  $(0,1)$  (see step 994 of figure 3.1). Now that the conditions of chaos have been visually satisfied with sensitive dependence on initial conditions and dense covering of the domain, we begin our chaotic analysis.

Flow of Initial Conditions for  $t(0)=0;tStep=\pi/2;h=205$

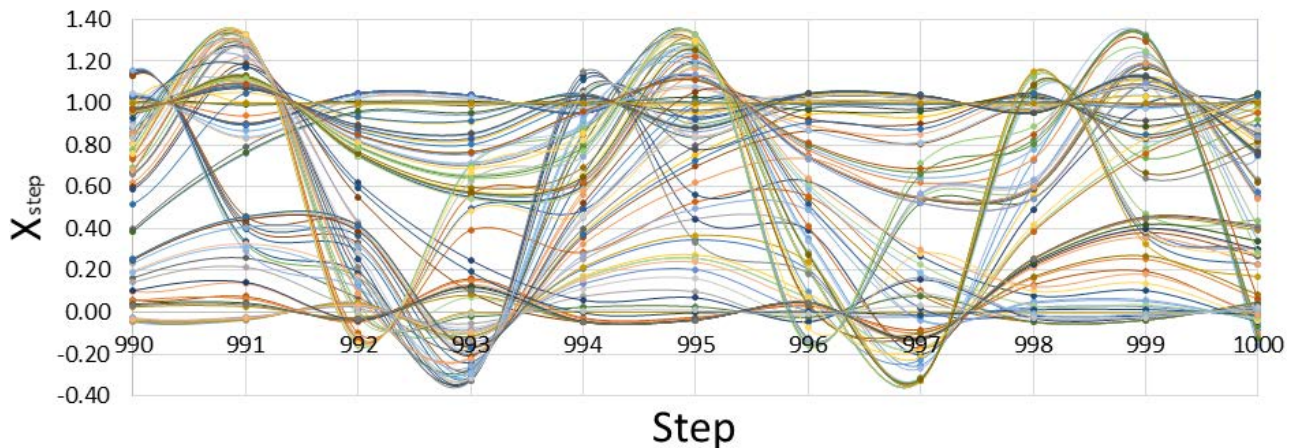


Fig. 3.1

However, if we zoom out a little and take a look at the behavior for 100 steps prior (fig 3.2), we notice that the system is apparently periodic on a global scale. Moreover, this system becomes unstable for different  $t(0)$  and therefore does not apply well to our motivation, as we must assume random initial conditions (i.e.  $t(0) = rand*2*pi$ ) in order for our system to be applied to a neural network. Therefore, not only is this system not entirely chaotic, it is not practical for our application. We will need to keep our  $h$  value under the global max to ensure the system is robust under any initial conditions.

Flow of Initial Conditions for  $t(0)=0;tStep=\pi/2;h=205$

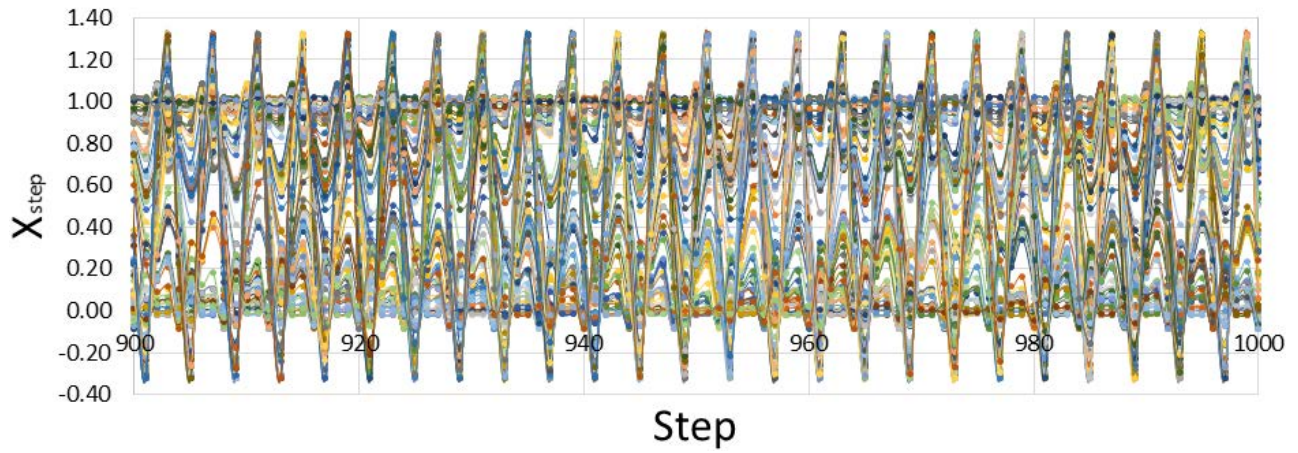


Fig. 3.2

Flow of Initial Conditions  $t(0)=rand;tStep=3;h=250$

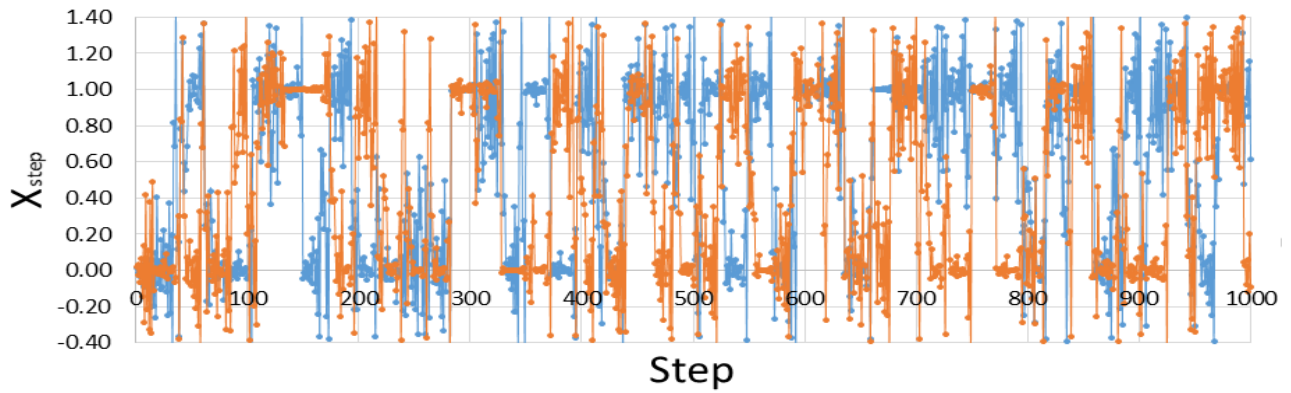


Fig. 3.3

Flow of Initial Conditions  $t(0)=rand;tStep=rand;h=190.5$

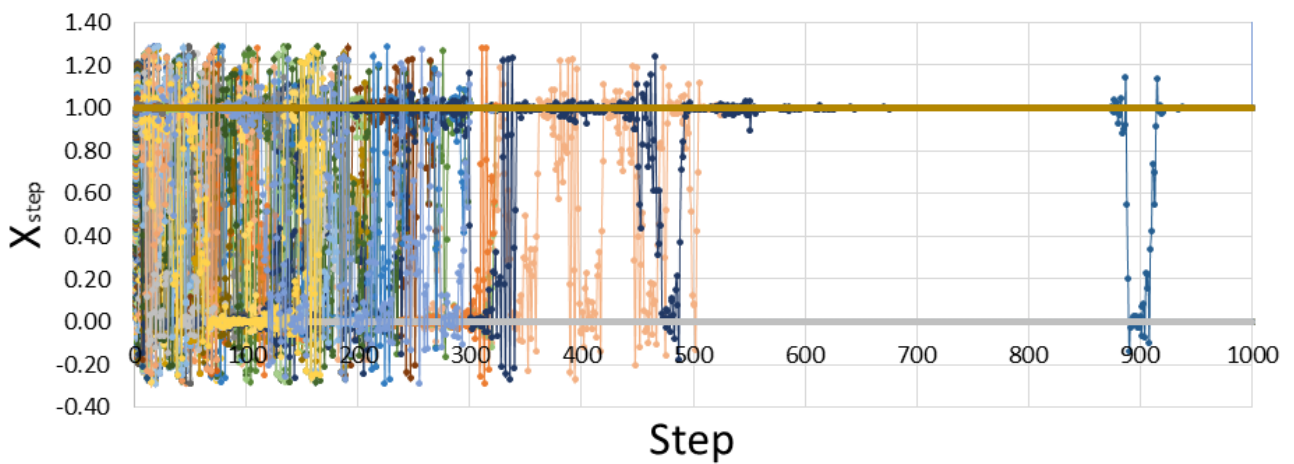


Fig. 3.4

When  $tStep$  is not a multiple of  $\pi$ , the aperiodicity is removed, and complete chaos ensues as  $t$  goes to infinity (fig 3.3). However, we are limited on our selection of  $t(0)$  and  $tStep$ . When  $h$  is set at 190.5 and  $tStep$  and  $t(0)$  are allowed to take on random conditions  $(0, 2\pi)$  transient chaos persists in the system. Furthermore, although the perturbation must be fairly large, a slight push away from the stable orbit will cause the trajectory to begin jolt off on another transiently chaotic orbit before stabilizing again on 0 or 1. In figure 3.4 a .01 perturbation was added to a random trajectory at step 867.

The kind of behavior pictured in figure 3.4 is what we are hoping to see based on the motivation of creating this dynamical system. Theoretically, the activations, plotted in figure 3.4 on the  $y$ -axis, are chaotically flowing through the system, and settle around points which provide the smallest loss,  $F(x, t)$ . However, small perturbations from back-propagation will destabilize a trajectory which has settled near at a non-optimal local minima. The paper will now transition to determining if there are some intervals of  $tStep$  that  $h$  could be increased without losing global stability for a random  $t(0)$ . We know that the system is globally stable at  $h = 190.5$ ; but what regions are “locally” stable for larger  $h$ ?

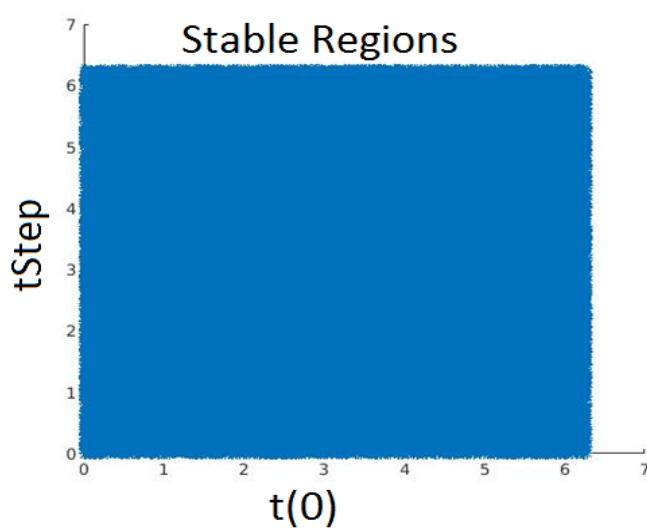


Fig 3.5  $h = 190.5$

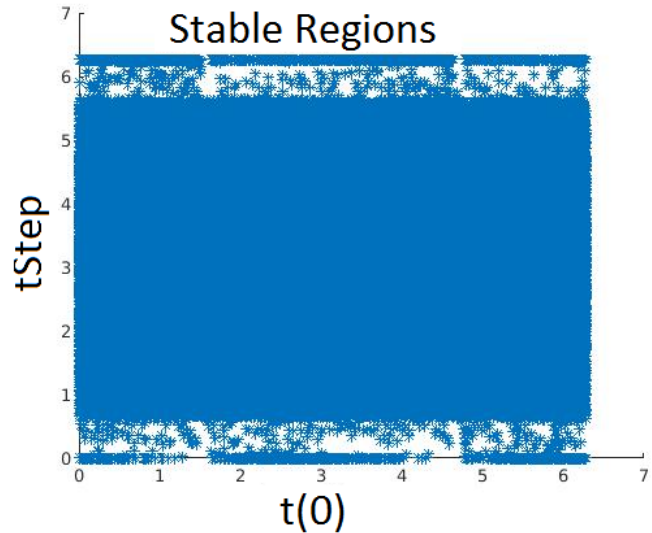


Fig. 3.6  $h = 191.0$

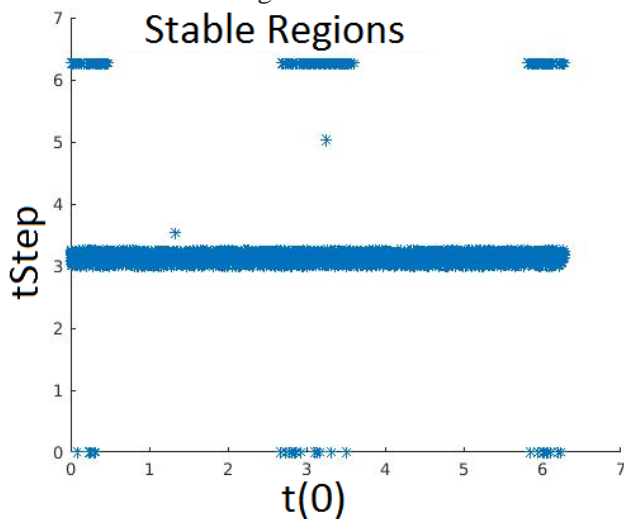


Fig. 3.7  $h = 265$

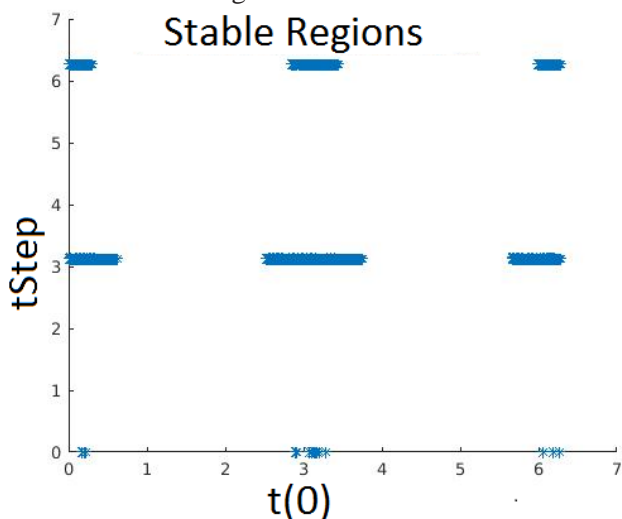


Fig. 3.8  $h = 300$

We see that the stable regions shrink to a volume of zero as  $h$  grows and is no longer visible at this resolution. We notice that the system is always stable within some interval of  $tStep = 0$  and  $\pi$  until  $h$  is greater than approximately 265. For larger  $h$ , the system is only stable for particular  $t(0)$ . Below we plot the valid  $x$  values vs their respective loss,  $F(x,t)$ , to examine the behavior further. Since we noticed something special about  $tStep = \pi$  we set it constant and plot the valid responses. We assume that there should be a positive  $\delta$  and  $\epsilon$ , where  $\delta = |N*\pi - \delta|$  ( $N$  a positive integer), that for any  $h$  if  $tStep < \delta$  the system will remain stable for all  $x_0 < \epsilon$  at any  $t(0)$ . The derivative of  $F(x,t)$  approaches 0 as  $\epsilon$  approaches zero. Therefore, we have a loose proof that although the volume of the region approaches to zero, there is some structure that remains.

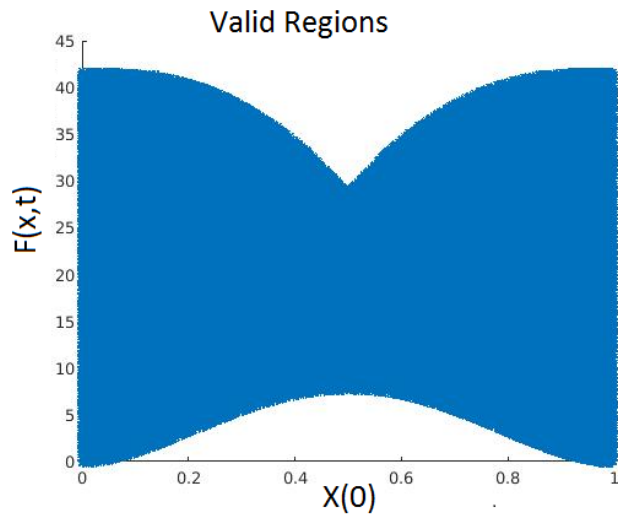


Fig. 3.9  $h = 190.5$

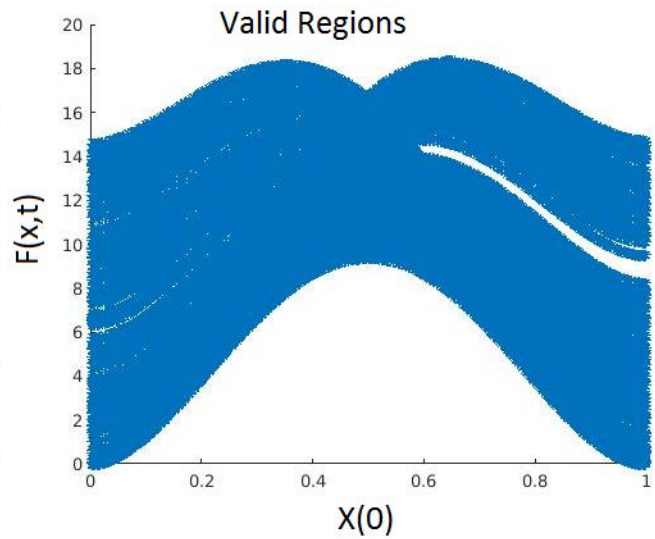


Fig. 3.10  $h = 191.0$

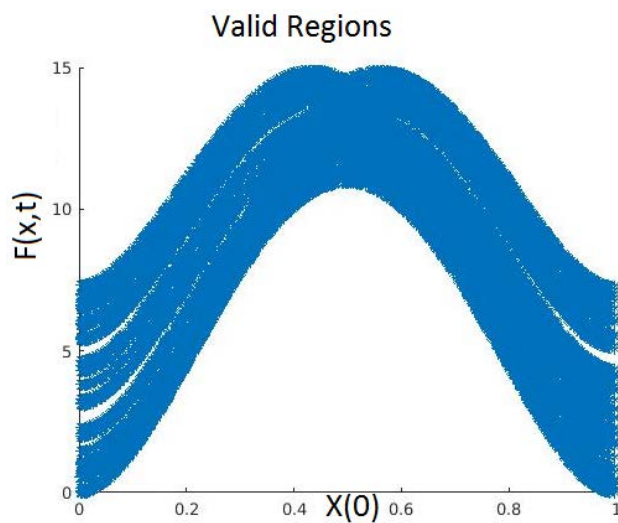


Fig. 3.11  $h = 265$

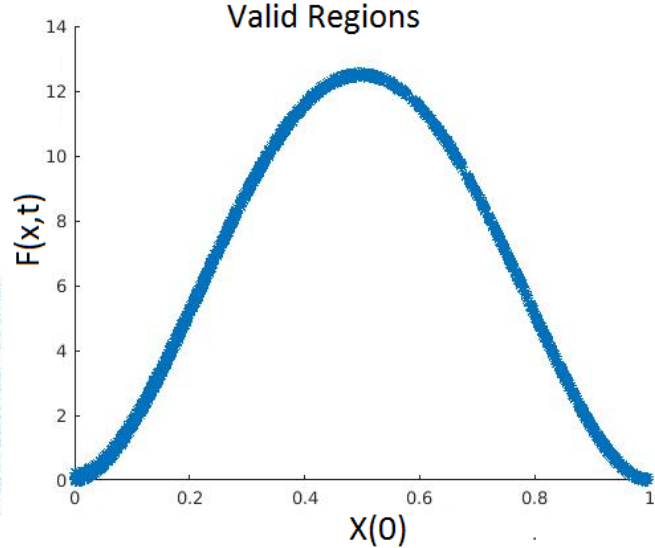


Fig. 3.12  $h = 300$

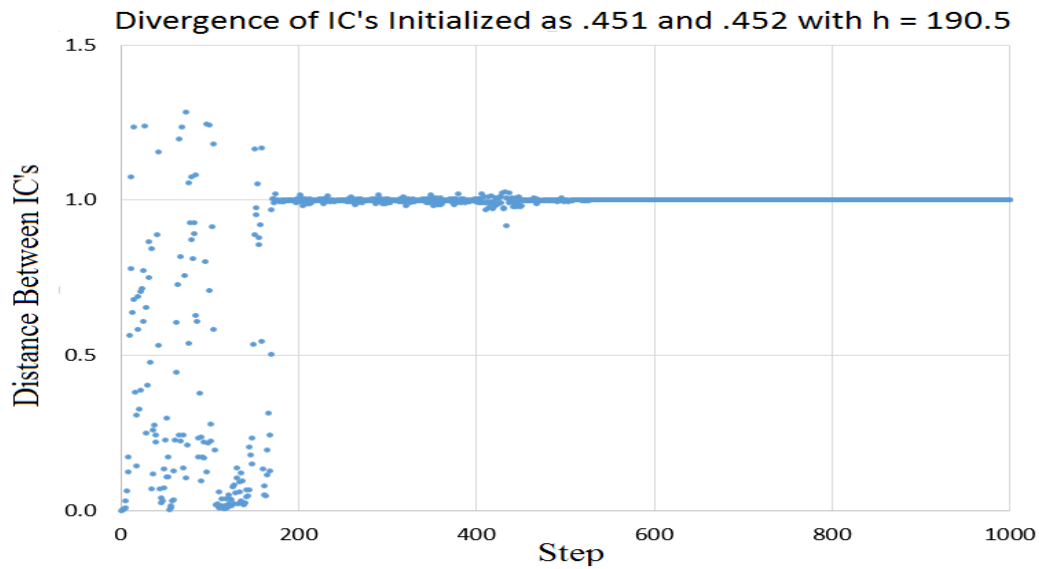


Fig 3.13 Transient chaos

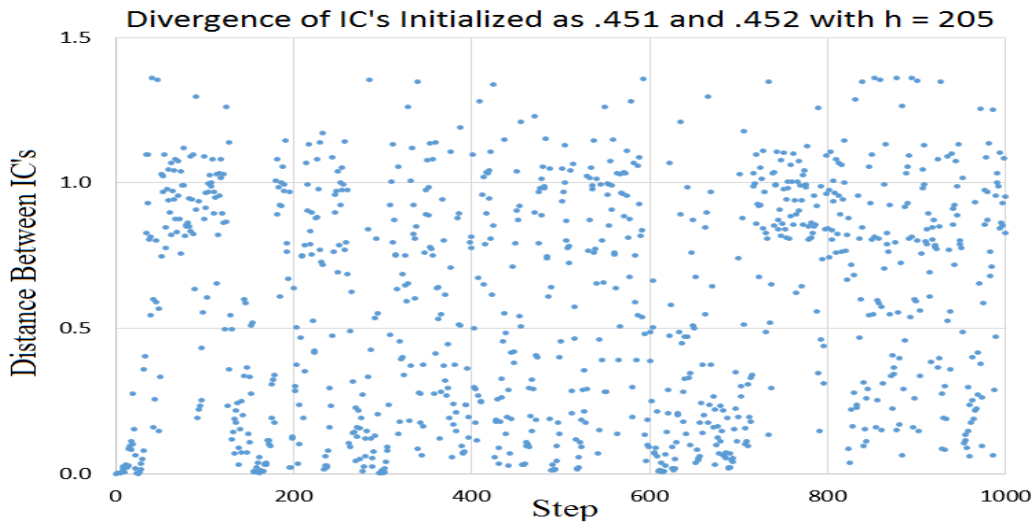


Fig. 3.14 Persistent chaos

Figure 3.13 visualizes the divergence and sensitive dependence of initial conditions when  $h$  is low enough that the orbits 0 and 1 are attractors. Figure 3.14 is a visual of when  $h$  is locally stable and chaos persists, but the system itself is a chaotic attractor.

## 4 Experiments

### 4.1 Stochastic Rounding

4.1 We began exploring how to experiment with our results by looking at **BinaryConnect**(BinaryConnect) and **BinaryNet**( BinaryNet). These papers do not attempt to modify the loss function, and instead use a stochastic binarization technique to train binary weight. Namely, the function BinaryConnect and BinaryNet use is a hard sigmoid, and name the process Stochastic Rounding, s.t.:

$$x^1 = \text{Sign}(x) = \begin{cases} +1 & \text{if } x \geq 0 \\ -1 & \text{otherwise} \end{cases}$$

$$x^1 = \begin{cases} +1 & \text{with probability } p = \sigma(x) \\ -1 & \text{with probability } 1 - p \end{cases}$$

$$\sigma(x) = (\text{clip}\left(\frac{x+1}{2}\right), 0, 1)$$

(BinaryNet)

From equation 1.2., treating t as a constant and solving for zero, we looked at the relative space that the equation had a positive, and negative value . We form the conjecture that the probability of rounding can be found as follows:

Solving for t in equation 1.2 we obtain:

$$t = \sin^{-1}(1 - 2x), \text{ and } t^* = \pi - t \text{ s.t. } t \ \& \ t^* \in [0, 2\pi)$$

Then our conjecture is that the probability to switch rounding is:

$$P(\text{switch}) = \frac{t^* - t}{2\pi} = \frac{1}{2} - \frac{t}{\pi} \tag{Conjecture 4.1}$$

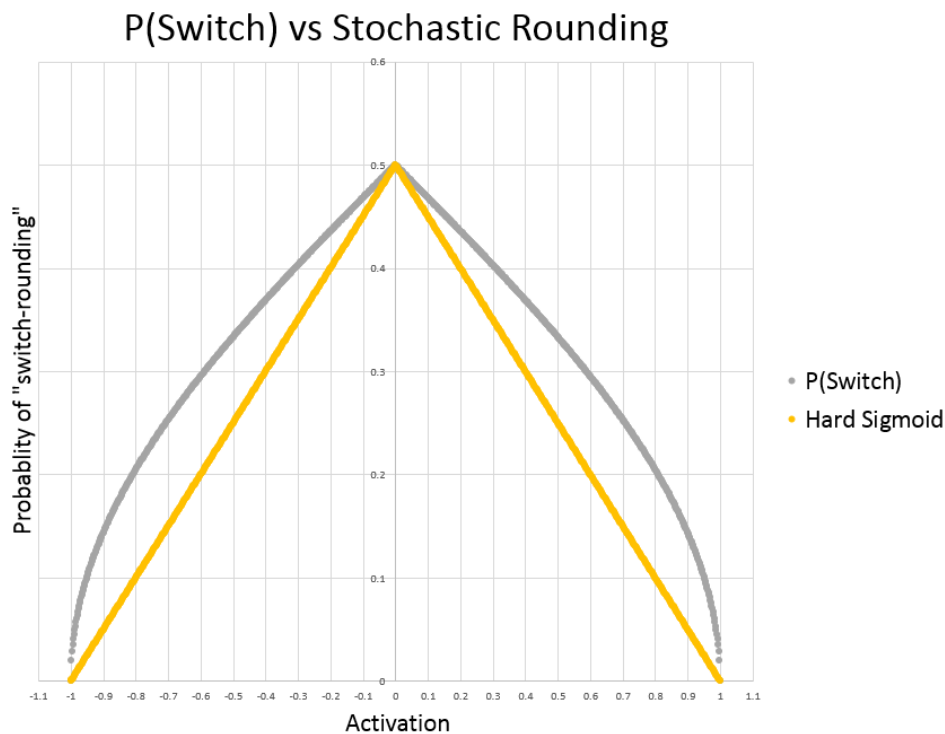


Fig. 4.1: Probability of switch rounding scaled [-1,1]

We implemented this new probability to BinaryNet and BinaryConnect with the following results:

Code Base:	BinaryNet				Binary Connect			
Version:	Original		P(Switch)		Original		P(Switch)	
Data Set:	CIFAR	MNIST	CIFAR	MNIST	CIFAR	MNIST	CIFAR	MNIST
Test Error:	11.39	.99	12.61	1.40	7.92	1.22	9.38	1.15

Table 4.1

While we only out-performed one of the four test sets, we believe there is room to explore optimal probability of switching in future work. The results also gave us promise that our research was progressing well and that adding equation 1.3 to the loss function of a neural network would produce positive results.

## 4.2 Dynamic Loss

The motivation for developing this equation was to create a binary layer which could be fed into a neuromorphic processor. Therefore, in our experiments we focus on changing a single layer of weights to have a binary representation and examine the results. We added equation 1.3 to the loss function in the TensorFlow “SoftMax” and “Deep” MNIST tutorials for baseline since there are limited works available that reference training through loss-function (TensorFlow). For the “SoftMax” model, we let the  $x$  from equation 1.3 be defined as the weights,  $W$ , of the network (there is only one layer) and rounded the weights off at the end of training. Less than 10 percent of the available weights took on values of 1, with the remainder taking 0. For the “Deep” model, we let the  $x$  from equation 1.3 be defined as the second convolutional layer weights,  $W_{conv2}$ , and rounded the weights off at the end of training. For both models we initialized  $t$  at one and increased  $t$  by one for every training step, and we initialized  $H$  at a locally stable value of 300.

We achieved positive results, losing less than one percent of test accuracy and obtaining a binary representation of the data at a layer. We believe this satisfies our initial research goal of developing function to transduce data for a neuromorphic processor. Our results follow:

Test Accuracy of Model	SoftMax	Deep
Original	91.60	99.16
Loss + Equation 1.3	90.70	99.01

Table 4.2

## 5 Conclusion

- (1) Is this system always predictable; does there exist sensitive dependence on the initial conditions (SDIC)?

We conclude that if  $160 > h$  that this system is always predictable. However, for  $h$  larger than 160 the system displays SDIC. If  $190 > h > 160$  the system is unpredictable, but is only transiently chaotic; trajectories have a steady end-state either orbiting or equal to 0 or 1.

- (2) How large is “too” large for parameter  $h$ ?

We conclude that  $h > 400$  makes the system unstable for nearly all initial conditions.

- (3) Are there parameters for which there exists chaos?

If  $400 > h > 191$  there are regions of initial conditions for which there is persistent chaos, but the system remains stable in the region for all initial conditions.

- (4) Can this function be added to the loss of a neural network to train transduction layers?

The function was added to the loss function with positive results. Although there are limited works available to compare our experiments against, we have shown that we can use a dynamic equation to entice a loss function to achieve a binary network.

## Bibliography

BinaryNet, arXiv 1602.02830. <https://arxiv.org/abs/1602.02830>.

BinaryConnect, arXiv 1511.00363. <https://arxiv.org/abs/1511.00363>.

Strogatz, Steven H., Nonlinear Dynamics and Chaos, page 373. Westview Press, 2015.

Pitt, arXiv 1604.00697. <https://arxiv.org/abs/1604.00697>.

TensorFlow, GitHub. <https://github.com/tensorflow/tensorflow/tree/r1.3/tensorflow/examples/tutorials/mnist>.